ELSEVIER

Ceramics International 31 (2005) 811–815

CERAMICS INTERNATIONAL

www.elsevier.com/locate/ceramint

# Preparation and sintering of Ni-coated $Si_3N_4$ composite powders

He Wanbao, Zhang Baolin*, Zhuang Hanrui, Li Wenlan

*Shanghai Institute of Ceramics, Chinese Academy of Sciences, Shanghai 200050, People's Republic of China*

Received 7 June 2004; received in revised form 30 June 2004; accepted 12 September 2004
Available online 16 December 2004

**Abstract**

Ni-coated $Si_3N_4$ composite powders were prepared successfully via electroless plating by using sodium hypophosphate ($NaH_2PO_2$) as reducing agent. The Ni coating layers contained 12 wt.% phosphor and were dominantly amorphous with a thickness of 20–60 nm. The sintering properties of Ni–$Si_3N_4$ composite were improved by adding $Mo_2C$ into $Si_3N_4$ powders, in which $Mo_2C$ formed liquid to improve the α–β transformation of $Si_3N_4$, and $Mo_2C$ converted into $MoSi_2$ after sintering. The composite powders were densified by hot-pressing at 1600 °C. The final crystal phases of the sintered samples were $Si_3N_4$, Ni and $MoSi_2$.

*Keywords:* D. Silicon nitride; Nickel; Molybdenum carbide

## 1. Introduction

Silicon nitride ceramics have been investigated as high-temperature materials for their excellent characteristics [1]. The wide use of silicon nitride is still limited due to its catastrophic fracture. By combining $Si_3N_4$ with metal phases homogeneously, materials with high fracture toughness can be achieved and the materials may also be processed by electrical discharge machining (EDM). For example, by mechanical alloying of Ti and $Si_3N_4$ mixture, a Ti–$Si_3N_4$ composite were prepared which could be deformed plastically at 1300 °C and its wear-resistance was also greatly improved as compared to $Si_3N_4$, thus it could be used in the fields of plastic working and anti-abrasion [2]. Nickel, with excellent corrosion-resistance and wear-resistance properties, may also be used as a ductile phase to improve toughness of brittle nitride.

In recent years, various coating methods have been developed, by which the uniformity of the components can be improved, which leads to the improvement of the sintering property and the stability of materials [3–5]. Electroless plating presents an easy and effective coating technique, which can be applied on almost all material surfaces, either conductive or nonconductive, and regardless of the size and shape of the substate [6–10].

In the present study, Ni-coated $Si_3N_4$ powders and their composites have been prepared through electroless plating and then sintered at relatively low temperature.

## 2. Experimental procedures

Homemade $Si_3N_4$ powders ($\alpha\% = 93$ wt.%, $D_{50} = 1.7$ um) were used for coating. The other reagents used in the experiment were all analytical-grade reagents. The compositions of the solutions and the processing conditions used are listed in Table 1. $Si_3N_4$ powders were first immersed into NaOH solutions, which resolved in the formation of micropores on the $Si_3N_4$ surfaces by erosion to increase the adsorptive capacity. This process is so called roughening. Then the roughened powders were immersed into acid stannous chloride ($SnCl_2$) solutions, in which $SnCl_2$ could hydrolyze into Sn(OH)Cl and be absorbed on the $Si_3N_4$ particles. This process can be called sensitizing. After that, the sensitized powders were immersed into the acid palladium chloride ($PdCl_2$) solutions, in which $Pd^{2+}$ reacted with Sn(OH)Cl to form Pd nuclei on the $Si_3N_4$ surfaces. The

---

* Corresponding author. Tel.: +86 21 52414322; fax: +86 21 52413903.
*E-mail address:* blzhang@mail.sic.ac.cn (Zhang Baolin).

0272-8842/$30.00 © 2004 Elsevier Ltd and Techna Group S.r.l. All rights reserved.
doi:10.1016/j.ceramint.2004.09.008

Table 1
The compositions of roughening, sensitizing, activating and electroless baths and process time

| | Roughening bath | Sensitizing bath | | Activating bath | | | Eletroless plating bath | |
|---|---|---|---|---|---|---|---|---|
| Reagents | NaOH (1 M) | $SnCl_2 \cdot 2H_2O$ | HCl (12 M) | $PdCl_2$ | HCl (12 M) | $NiCl_2 \cdot 6H_2O$ | $NaH_2PO_2 \cdot H_2O$ | $Na_3C_6H_5O_7 \cdot 2H_2O$ |
| Concentration | 10 ml/g | 20 g/l | 40 ml/l | 0.20 g/l | 2.5 ml/l | 52 g/l | 51 g/l | 30 g/l |
| Process time | 30 min | 5–10 min | | 3–5 min | | | 30 min | |

Pd nuclei will act as the cores of crystallization during electroless plating. After this so called activating process, $Si_3N_4$ powders were immersed into the electroless plating solutions for coating at 40 °C. During the process, all solutions were stirred with an electromagnetic stirrer to avoid particle settling, and powders were thoroughly rinsed using de-ionized water in every step to prevent contamination of solutions. In every batch 40 g/l $Si_3N_4$ powders were processed in the electroless plating solutions for 30 min.

The as-prepared composites powders were then hot-pressed in the atmosphere of $N_2$ at 1600 °C for 1 h under uniaxial pressure of 16 MPa.

The morphologies of initial and as-coated powders were characterized by transmission electron microscopy (TEM) (JEM200CX). The chemical compositions of the coated powders were determined by X-ray fluorescence spectroscopy (XRF). The phase compositions were determined by X-ray diffractometry (XRD).

The morphologies and elements distributions of sintered samples were determined by backscattered electron image (BSE). The bulk density was determined using Archimedes principle. The bending strength ($\sigma_f$) was determined by three-point bending method, and the fracture toughness ($K_{IC}$) was determined on indentation hardness tester.

## 3. Results and discussion

### 3.1. The preparation and characterization of the composite powders

The morphologies of the initial powders and as-coated powders are shown in Fig. 1. The initial powders showed a clean surface of grains, while the grains of the as-coated powders were surrounded by small particles. The coatings distributed on all areas of the $Si_3N_4$ grains regardless of their size and shapes. The thickness of the coating layers is estimated to be 20–60 nm according to the TEM pictures (Fig. 1). To further determine the coating results, the coated powders are inlaid and polished, the cross-section of the coated powders were observed by BSE. In Fig. 2, the dotted arrow points to a uniform bright layer, which is the characteristic of metal phase. In connection with the XRD analysis (Fig. 3) the bright layer is identified as Ni. The solid arrow points to a $Si_3N_4$ grain. Fig. 2 indicates that $Si_3N_4$ was coated with a uniform Ni layer, and the XRF results indicate that both Ni and P existed in the coated powders, and there are 12 wt.% phosphors in the coating alloys (Table 2). This was because of the use of $NaH_2PO_2$ as the reducing agent. A broadened peak at around $2\theta = 45^\circ$ can be seen in XRD pattern (Fig. 3), and this is the typical pattern of amorphous materials. This result is consistent with previous studies that electroless nickel deposits may have structures from extremely small crystallites to fully amorphous [10] and Ni–P alloys with more than 8 wt.% phosphors are dominantly amorphous [10,11].

### 3.2. Sintering of the composite powders and characterization of sintered samples

The as-prepared composites powders were hot-pressed in the atmosphere of $N_2$ at 1600 °C for 1 h under uniaxial pressure of 16 MPa. In the sintering 10 wt.% $Mo_2C$ was added to improve the densification.

The bulk density of the sintered samples was 3.32 g/cm$^3$, the bending strength ($\sigma_f$) was 403 ± 3MPa, and the fracture

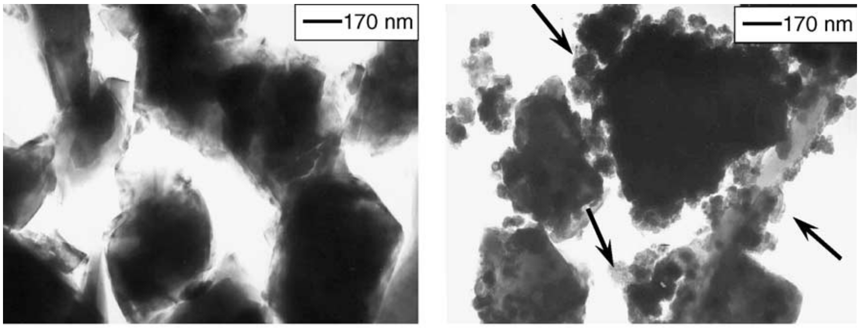

(a) TEM pictures of initial powders (b) TEM pictures of coated powders

Fig. 1. The morphologies of the initial (a) and as-coated (b) powders.

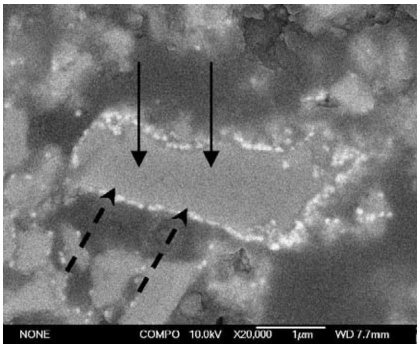

Fig. 2. BSE pictures of a coated particle.

Table 2
XRF results of the coated powders

| Components | Contents (%) |
|---|---|
| $Si_3N_4$ | 81.5 |
| P | 2.2 |
| Ni | 16.1 |
| Sn | 0.12 |
| Pd | 0.04 |

toughness($K_{IC}$) was $7.4 \pm 0.1$ MPa m$^{1/2}$. XRD results (Fig. 4a) show that in the samples only β-$Si_3N_4$, Ni and $MoSi_2$ could be identified. The initial α-$Si_3N_4$ has been all converted into β-$Si_3N_4$, and $Mo_2C$ disappeared while $MoSi_2$ is observed.

To investigate the role of $Mo_2C$ in the sintering of $Si_3N_4$–Ni composites, 84 wt.% $Si_3N_4$–16 wt.% Ni and 89.4 wt.% $Si_3N_4$–10.6 wt.% $Mo_2C$ were prepared according to the same proportions in the sintered $Si_3N_4$–Ni–$Mo_2C$ composites. XRD results show that β-$Si_3N_4$ and α-$Si_3N_4$ are present in the 84 wt.% $Si_3N_4$–16 wt.% Ni composites (Fig. 5a) and there is still 64 wt.% α-$Si_3N_4$ in the composite. No Ni and Ni–Si compounds peaks in the XRD pattern are found. β-$Si_3N_4$, α-$Si_3N_4$ and α-$Mo_2C$ are present in the 89.4 wt.% $Si_3N_4$–10.6 wt.% $Mo_2C$ composites (Fig. 5b), which indicates that without Ni $Mo_2C$ did not react with $Si_3N_4$ to form $MoSi_2$ at 1600 °C and the generation of $MoSi_2$ in $Si_3N_4$–Ni–$Mo_2C$ is due to the presence of Ni. There is still 66 wt.% α-$Si_3N_4$ in the $Si_3N_4$–$Mo_2C$ composite. As for Ni–$Mo_2C$, Ni and $Mo_2C$ form a solid solution below 1250 °C and becomes liquid above 1250 °C [12].

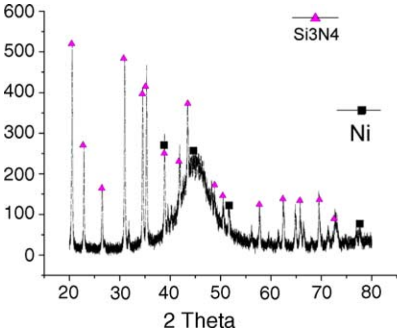

Fig. 3. XRD pattern of the coated particles.

The sintering mechanism can be that during the sintering $Mo_2C$ first form Ni–$Mo_2C$ solid solution below 1250 °C, and above 1250 °C, liquid phase appears and the liquid is important for the α-$Si_3N_4$ transformation to β-$Si_3N_4$. Meantime, the liquid reacts with $Si_3N_4$ to form $MoSi_2$.

The BSE pictures (Fig. 6) show that there are three contrast grades in the composite. In the bright areas (point 1) there are mainly Si, Mo and a little Ni, while the dark areas (point 2) are the main crystal grains containing mainly Si element, and in the brighter areas (point 4) there are mainly Si, Mo, Ni and P. In connection with the XRD result (Fig. 4a), the phases in the dark, bright and brighter areas are β-$Si_3N_4$, $MoSi_2$ and $MoSi_2$ with Ni, respectively. In the sintered composite, β-$Si_3N_4$ was the main phase, Ni and $MoSi_2$ were distributed on the grain boundaries of β-$Si_3N_4$.

The morphologies of the fracture surface (Fig. 4b) indicate that $Si_3N_4$ did not form rod-like crystals and the crystal grains were small and bonded to each other. The fracture mode of the composites was transcrystalline rupture.

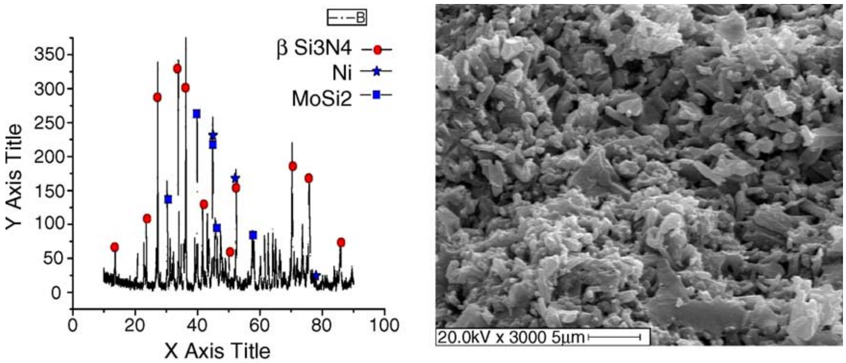

(a) The XRD pattern (b) The morphology of the fracture surface

Fig. 4. The XRD pattern (a) and the morphology of the fracture surface (b) of sintered $Si_3N_4$–Ni–10% $Mo_2C$.

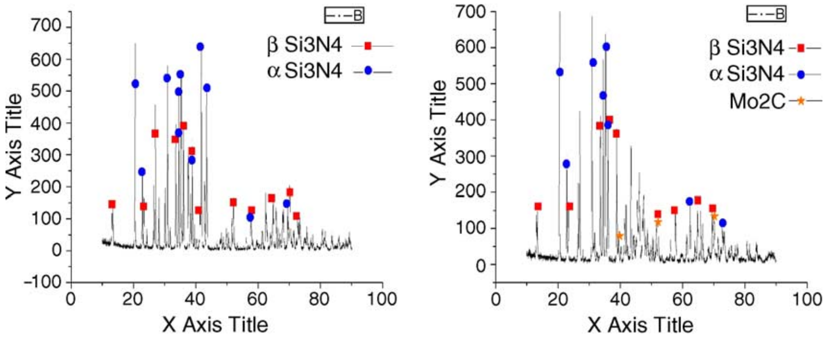

(a) 84wt%$Si_3N_4$-16wt%Ni (b) 89.4wt%$Si_3N_4$-10.6wt%$Mo_2C$

Fig. 5. The XRD pattern of sintered 84 wt.% $Si_3N_4$–16 wt.% Ni (a) and 89.4 wt.% $Si_3N_4$–10.6 wt.% $Mo_2C$ (b).

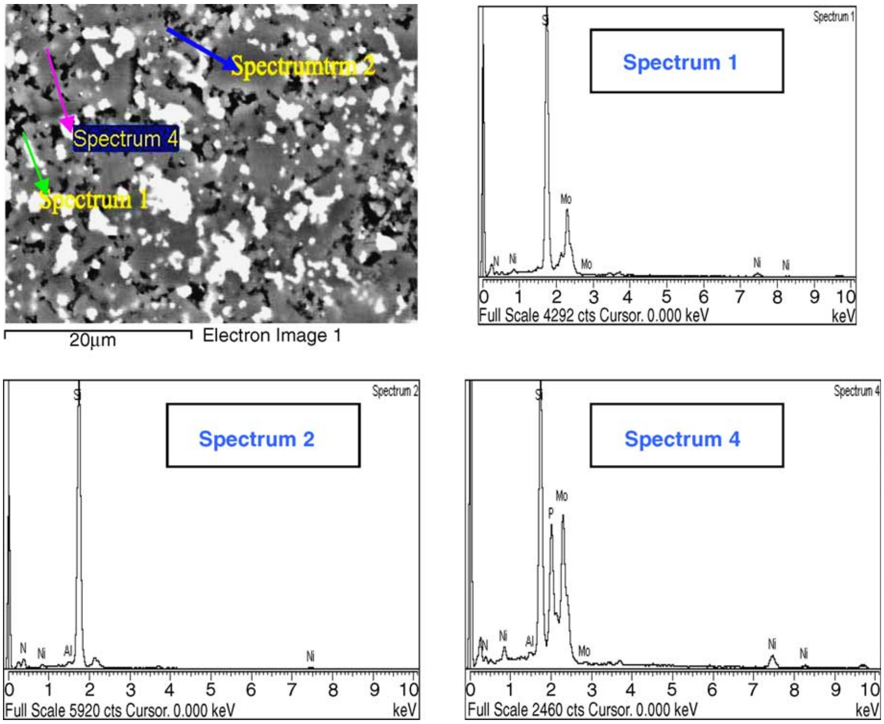

Fig. 6. The BSE pictures of sintered $Si_3N_4$–Ni–10% $Mo_2C$.

## 4. Conclusions

(1) Ni-coated $Si_3N_4$ powders could be prepared via the electroless plating of nickel on $Si_3N_4$ particles. The electroless nickel layers contained 12 wt.% phosphors and were dominantly amorphous. The thickness of the nickel coating layers was 20–60 nm.

(2) $Mo_2C$ improved the sintering properties. The bulk density of the sintered samples was 3.32 g/cm$^3$, the bending strength ($\sigma_f$) was 403 ± 3 MPa, and the fracture toughness ($K_{IC}$) was 7.4 ± 0.1 MPa m$^{1/2}$. The fracture mode of the composites was transcrystalline rupture.

(3) The phases of the sintered samples were $Si_3N_4$, Ni and $MoSi_2$. β-$Si_3N_4$ was the main phase and Ni and $MoSi_2$ were distributed on the grain boundaries of β-$Si_3N_4$. During the sintering, Ni–$Mo_2C$ first formed liquid, then α–β transformation of $Si_3N_4$ occurred in the liquid, the liquid reacted with $Si_3N_4$ to form $MoSi_2$ after sintering.

## References

[1] M.J. Hoffmann, G. Petzow, Microstructure design of $Si_3N_4$ based ceramics, in: I.-W. Chen, P.F. Becher, G. Petzow, T.S. Yen (Eds.), Silicon Nitride Ceramics Scientific and Technology Advances, Materials Research Society, Pittsbugh, PA, 1993, pp. 3–14.

[2] M. Nawa, T. Sekino, K. Niihara, J. Mater. Sci. 29 (1994) 3185.

[3] H. Giesche, J. Dispersion Sci. Technol. 19 (1998) 249–265.

[4] C.Y. Yang, W.H. Shih, J. Am. Ceram. Soc 82 (1999) 436–440.

[5] W.H. Tuan, H.H. Wu, T.J. Yang, J. Am. Ceram. Soc. 30 (1995) 855–859.

[6] A.A. Khan, J.C. Labble, J. Eur. Ceram. Soc. 17 (1997) 1885.

[7] S. Vives, C. Guiazard, L. Cot, C. Oberlin, J. Mater. Sci. 34 (1999) 3127.

[8] T. Sekino, T. Nakajima, S. Ueda, K. Niihara, J. Am. Ceram. Soc. 80 (1997) 1139.

[9] O.H. Sung-Tag, S. Mutsuo, N. Koichi, J. Mater. Sci. 36 (2001) 1817–1821.

[10] Y.K. Jeong, A. Nakahira, P.E. Morgan, K. Niihara, J. Mater. Sci. 80 (1997) 1307.

[11] G. Carotenuto, A. Gallo, L. Nicolais, Appl. Comp. Mat. 1 (1994) 231.

[12] G.P. Dmitrieva, N.A. Razumova, A.K. Shurin, Sov. Powder Metall. Met. Cera 23 (1984) 714–718 (English Translation).